Percolation-like transition in DLA with two species

1996 J. Phys. A: Math. Gen. 29 1905

(http://iopscience.iop.org/0305-4470/29/9/007)

J. Phys. A: Math. Gen. **29** (1996) 1905–1913. Printed in the UK

Percolation-like transition in DLA with two species

Jean-Marc Debierre† and Gilbert Albinet‡

† Laboratoire MATOP§, Case 151, Université d'Aix-Marseille III, Faculté des Sciences et Techniques de Saint-Jérôme, 13397 Marseille Cedex 20, France

‡ Institut de Recherche sur les Phenomenes Hors Equilibre‖, Case 252, Université d'Aix-Marseille I et II, Faculté des Sciences et Techniques de Saint-Jérôme, 13397 Marseille Cedex 20, France

Received 6 November 1995

Abstract. We introduce a DLA model with two species in order to simulate the growth of alternate clusters. We perform intensive numerical simulations in two dimensions in which the proportions of the two species are varied. A critical point, analogous to a percolation threshold, is found and a new class of critical exponents is obtained for this transition. Within numerical accuracy, the fractal dimension of the clusters is found to be the same as in the usual DLA model, independent of the species concentrations. Possible connections with the growth of two-dimensional ionic crystals are discussed.

1. Introduction

The diffusion-limited aggregation (DLA) model originally introduced by Witten and Sander [1, 2] provides a unified description for a broad class of chemico-physical phenomena [3]. In the present paper, we introduce a similar model for the diffusion-limited aggregation of two species, A and B, with the imposed alternate condensation order A–B–A–B–A–B–.... This type of order governs the atomic or molecular structure of numerous materials, such as ionic crystals and certain binary alloys or gels.

In this paper, particular attention is devoted to the influence of the relative proportions, p and $1-p$, of the two species, A and B, which are varied in the numerical simulations. A cluster is the result of two mechanisms: diffusion and chemical aggregation. The second mechanism makes the system close to the A–B percolation problem which is known to behave like regular percolation [4]. So, a DLA-like fractality and a percolation-like criticality mingle in this model.

The paper is organized as follows. The model is briefly described in section 2. In section 3, the results for $p = \frac{1}{2}$ are discussed, numerical evidence for the existence of a critical point, $p = p_c$, are given and the subcritical regime, $p < p_c$, is studied. Concluding remarks are finally presented in section 4.

2. Model

The model is defined on a square lattice whose sites are represented by pairs (x, y) of integer coordinates. The origin $(0, 0)$ is placed at the centre of the lattice. Initially, all

§ Unité de Recherche Associée au CNRS 1530.

‖ Unité Mixte de Recherche CNRS 138.

0305-4470/96/091905+09$19.50

the lattice sites are empty, except for $(0, 0)$ and $(1, 0)$ which are occupied by an A and a B particle, respectively. This two-particle cluster starts to grow by the addition of new incoming particles.

A regular DLA algorithm [3] is used and no difference is made for the diffusion of an A or a B particle. The motion of a free particle is controlled by two fictitious circles: they are defined before each launching, centred at $(0, 0)$, with radius R_1 and R_2 ($R_1 < R_2$). We set $R_1 = R_{\max} + 5$, where $R_{\max}$ is the maximum radius corresponding to the outermost tip of the cluster and $R_2 = 10R_1$. When the particle reaches the perimeter of the largest circle, it is removed and launched again, from a randomly chosen point on the perimeter of the smaller circle. This method simulates the motion of a particle which diffuses far from the aggregate and returns close to it after a long time has elapsed.

To generate alternate clusters, a diffusing $A(B)$ particle is added to the cluster (i.e. crystallizes) only when it comes into contact with a previously crystallized $B(A)$ particle. Conversely, if an $A(B)$ diffusing particle reaches an $A(B)$ crystallized particle, it does not crystallize and keeps diffusing.

Each time a particle is added to the cluster, the next particle to crystallize is randomly chosen to be either an A particle with probability p or a B particle with probability $1 - p$. This particle diffuses until it crystallizes. For very low p values, we expect that the cluster rapidly saturates, with a B layer around it. If a B ion is chosen to be added next, it will never be able to crystallize and diffusion will go on forever. To overcome this difficulty, we had to limit the number α of attempts a given particle makes to crystallize to a maximum value $\alpha_{\max}$. For a N-particle cluster, $\alpha_{\max}$ was chosen to be of the order of N, since most of the particles belong to the perimeter and we want to explore the growth-site set. Test runs with $\alpha_{\max} = \max(5N, 100)$ and $\alpha_{\max} = \max(N, 100)$ gave very similar results so that the second limit was retained in the simulations. When α reached $\alpha_{\max}$, growth was stopped and the corresponding cluster was stored in a list of finite clusters.

Let us note that, on average, a particle encounters the cluster several times before sticking. Thus, our algorithm falls in the class of DLA with a sticking probability smaller than one [2] but this probability is not a constant in our case. This algorithm is of the order of N^2, whereas a regular DLA algorithm is of the order of N. For this reason, the maximum cluster mass N is set to a modest value, $N_{\max} = 8192$ (or less), in the simulations. The clusters that stop growing before reaching $N_{\max}$ are called closed clusters and the others are called open clusters. Since the present model is by definition symmetrical about $p = \frac{1}{2}$, we will assume that $p \leqslant \frac{1}{2}$ in the following.

3. Numerical results

For $p = \frac{1}{2}$. We first investigated the case of an equal proportion of A and B particles. We constructed a fairly large number (2×10^5) of small clusters ($N_{\max} = 256$). We found that the fraction $F(N)$ of clusters with a mass larger than N decreases exponentially and rapidly saturates to a constant value (figure 1). This result shows that about 75% of the clusters will grow indefinitely in this case.

To compute the fractal dimension of the open clusters, we constructed 1000 open clusters of mass $N = 8192$ (see figure 2) and used the sandbox method. Figure 3 is a log–log plot of the mass N as a function of the radius R. The data points for $R < 100$ correspond to the so-called frozen zone of the cluster, where growth is almost fully completed. A linear fit to the data points in this range gives $D = 1.67 \pm 0.01$, a value very similar to that found for regular DLA [5]. Above $R = 100$, the curve bends, since the data concern the active zone where growth is still important.

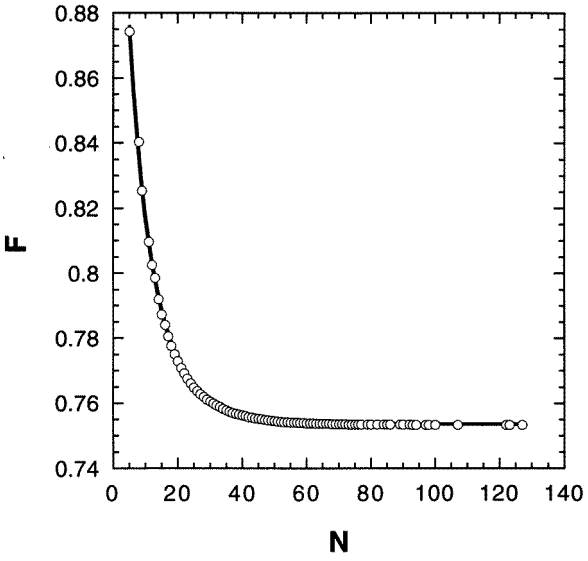

Figure 1. The variations of the proportion F of clusters with a mass greater than N at $p = \frac{1}{2}$. The full curve is a fit of the data points (open circles) to a curve of the equation $y = \alpha + \beta \exp(-\gamma x^{\delta})$, giving $\alpha \simeq 0.75$.

Figure 2. An 8192-particle open cluster grown at $p = \frac{1}{2}$.

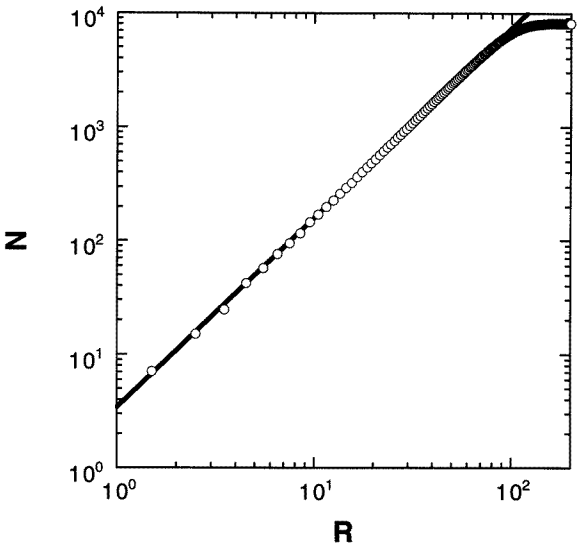

Figure 3. N versus R for the open clusters constructed at $p = \frac{1}{2}$. The full line is a linear fit of the data points and its slope is equal to $D = 1.67 \pm 0.01$.

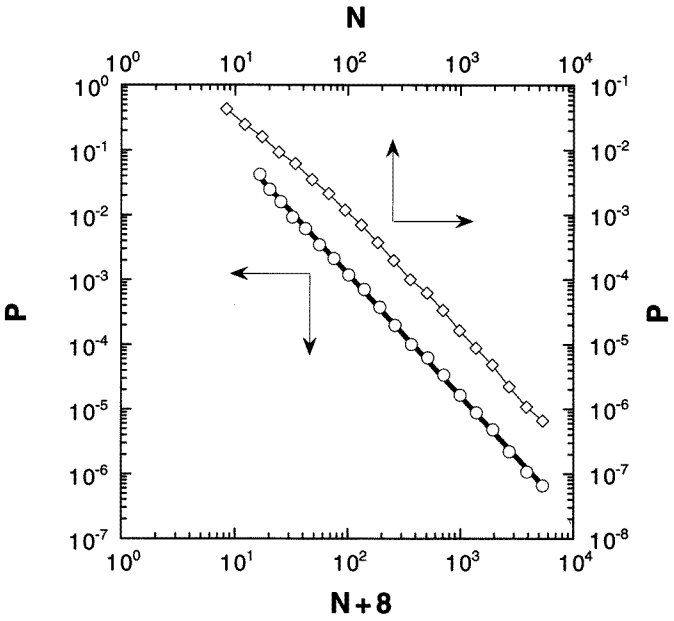

Figure 4. P plotted as a function of N (top and right axes) and as a function of $N + 8$ (bottom and left axes) at $p = 0.293$ ($N > 5$). The finite-size effects are notably lowered in the second case.

For $p \leqslant p_c$. We have just seen that for $p = \frac{1}{2}$ the probability for a cluster to remain open forever is non-zero. Now, the probability that a cluster reaches a given mass N ($N > 5$) obviously vanishes as $p \to 0$. We thus expect that there exists a critical probability p_c which delimits a finite cluster growth regime (for $p < p_c$) and an infinite cluster growth regime (for $p > p_c$). The former regime is studied in this paragraph. The transition which occurs at $p = p_c$ is somewhat reminiscent of percolation and will be analysed in close analogy with this well known model [6]. In particular, we will adapt here an analysis made in the context of tricolour percolation [7].

In order to determine the nature of the transition, the cluster mass distribution was computed for different p values. Let $P(N)$ be the probability to construct a cluster of mass N: it is simply defined as the number of N-particle clusters divided by the total number of clusters constructed. A characteristic cluster mass, N^*, is easily deduced from $P(N)$, as explained below. N^* increases continuously as p increases from zero and it diverges at the critical probability $p = p_c$, where

$$P(N) \sim N^{1-\tau}(1 + A/N)\,. \tag{1}$$

The A/N factor has been introduced to account for the finite-size corrections which are observed (figure 4).

When $p < p_c$, self-similarity is present up to a length scale $\xi \sim N^{*1/D}$, where D is the fractal dimension. Then, $P(N)$ is given by

$$P(N) = N^{1-\tau}(1 + A/N)f(X) \tag{2}$$

where X is the reduced variable N/N^* and $f(X)$ is a monotonic scaling function which tends towards a finite value when $X \to 0$ and to zero when $X \to \infty$, in order that $P(N)$ remains finite.

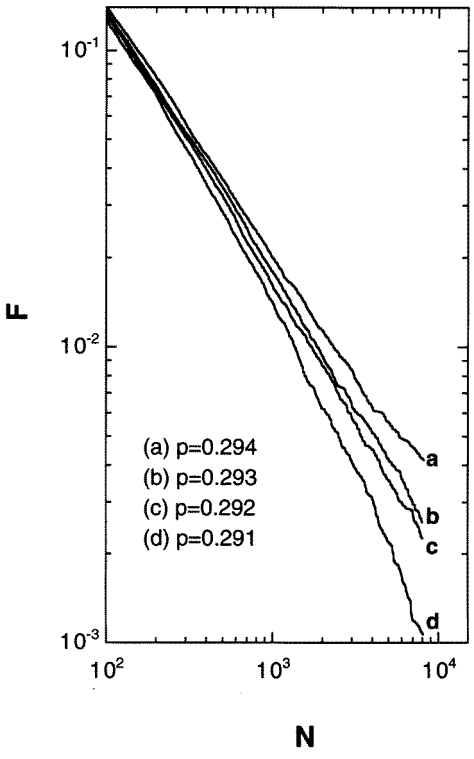

Figure 5. Evolution of $F(N)$ near the critical point p_c.

The cumulated probability F is defined as

$$F(N) = \int_N^\infty P(N')\,\mathrm{d}N' . \tag{3}$$

At $p = p_c$, the asymptotic behaviour of F should thus be

$$F(N) \sim N^{2-\tau} . \tag{4}$$

When p departs from p_c, according to (2) and (3), $F(N)$ will deviate from the simple power law given in (4), in the range $N > N^*$. More precisely, $F(N)$ must fall off exponentially when $p < p_c$ and asymptote to a non-zero constant for $p > p_c$. Figure 5 is a log–log plot of F as a function of N, for $p = 0.291$, 0.292, 0.293 and 0.294. The data points have been obtained by constructing 30 000 clusters with a cut-off mass $N_{max} = 8192$ for each p value. The best linear fit, obtained for $p = 0.293$, extends over two decades, which is a good criterion to determine p_c accurately. Our final estimate for the critical point is thus $p_c = 0.293 \pm 0.001$. The slope of the curve for $p = 0.293$ gives

$$\tau = 2.92 \pm 0.06 \tag{5}$$

the error bar being due mainly to the error on p_c.

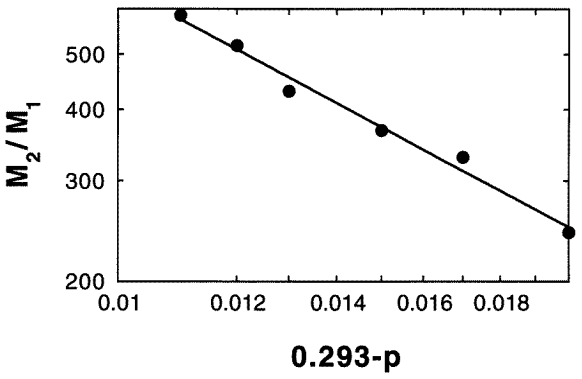

Figure 6. (M_2/M_1) plotted as a function of $(p_c - p)$. The full line is a linear fit of the data points. The slope is equal to -1.40 ± 0.09.

A direct plot of $\log P$ as a function of $\log N$ is curved on a rather wide range of small N values (figure 4). This curvature is due to the finite-size effects which are represented by the corrective term A/N in (1). It is easy to show that (1) is approximately equivalent to $P(N) \sim (N + N_0)^{1-\tau}$, a form which is easier to use in practice. We varied N_0 and found that the best choice is $N_0 = 8$, in order to bring the data points for $N > 5$ on a straight line (figure 4). The curve is now linear over about three decades, with a slope $1 - \tau = -1.89$, a result which is consistent with the above estimate for τ.

Next, we turned to the behaviour of the characteristic cluster mass N^* in the range $p < p_c$. We constructed 10^5 clusters for each of the six following values of p: 0.273, 0.276, 0.278, 0.280, 0.281, 0.282. All the clusters constructed are closed, so that the mass distribution is not biased by the cut-off N_{max}.

To compute N^*, we first define the two moments

$$M_1(p) = \int_{N_s}^{\infty} N' P(N')\, \mathrm{d}N' \tag{6}$$

and

$$M_2(p) = \int_{N_s}^{\infty} N'^2 P(N')\, \mathrm{d}N' \tag{7}$$

where $N_s = 5$ is the mass of the smallest clusters. Using equation (2), the integration of these expressions gives

$$M_1(p) \simeq K_1 + K_1' N^{*(3-\tau)} \tag{8}$$

and

$$M_2(p) \simeq K_2 N^{*(3-\tau)} + K_2' N^{*(4-\tau)}\,. \tag{9}$$

Sufficiently close to p_c, we have $N^* \to \infty$, so that

$$N^*(p) \simeq M_2(p)/M_1(p)\,. \tag{10}$$

In analogy with percolation theory, we expect that

$$N^*(p) \sim (p_c - p)^{-1/\sigma} \tag{11}$$

when $p \to p_c^-$. Figure 6 is a plot of M_2/M_1 as a function of $p_c - p$, on logarithmic scales. In order to take into account the inaccuracy on p_c, a linear fit was performed for $p_c = 0.292, 0.293$ and 0.294 and we obtained

$$\sigma = 0.71 \pm 0.10\,. \tag{12}$$

As a consistency check, the scaling function $f(X)$ defined in (2) was plotted in figure 7. The x and y coordinates represent $N/(M_2/M_1) \simeq X$ and $(N+8)^{\tau-1}P(N) \simeq f(X)$, respectively. The good collapse of the data points gives additional support to the results obtained so far.

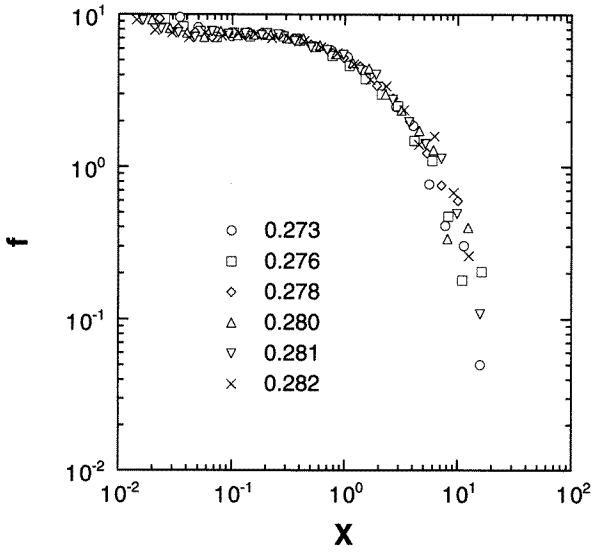

Figure 7. The scaling function $f(X)$ deduced from $P(N)$ for $N > 5$. The p values corresponding to the different sets of data points are given in the picture frame.

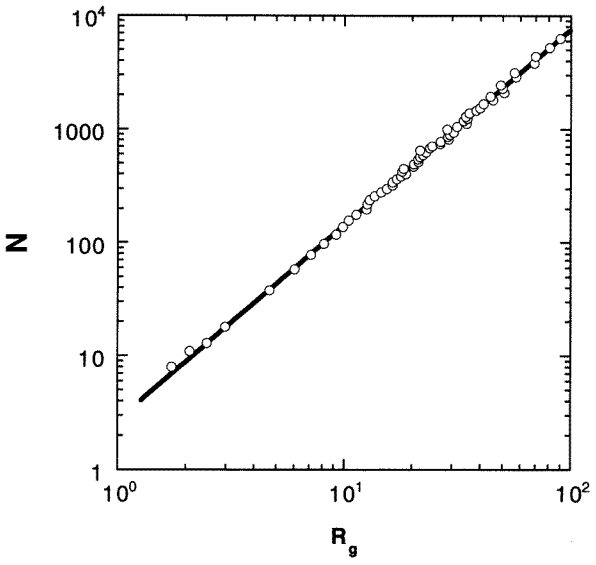

Figure 8. N versus R_g at $p = p_c = 0.293$. The full line is a linear fit of the data points.

Lastly, we looked at the influence of the critical point on the fractal dimension of the clusters. Figure 8 is a log–log plot of the cluster mass N as a function of the mean radius of gyration R_g. The data are extracted from 30 000 clusters constructed at $p = p_c = 0.293$. We obtain quite a linear curve, with a slope

$$D = 1.725 \pm 0.003\,. \tag{13}$$

This value is comparable to the estimate $D = 1.67 \pm 0.01$ found with a different method at $p = 0.5$. Since $\xi \sim (p_c - p)^{-\nu} \sim N^{*1/D}$, equation (11) gives

$$\nu = 1/(\sigma D) = 0.81 \pm 0.20 \tag{14}$$

for the critical exponent ν of the correlation length ξ. The set of critical exponents obtained (equations (5), (12) and (14)) defines a new universality class.

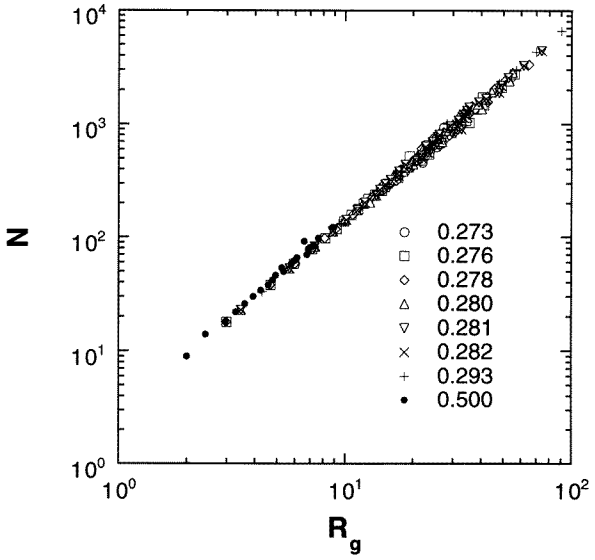

Figure 9. N plotted as a function of R_g for different p values given in the picture frame. Clearly, the whole set of data points falls on a single line.

The N versus R_g plots for the closed clusters obtained for all the p values considered are displayed in figure 9. This figure confirms that not only D, but also R_g does not depend on p for the clusters of size $R_g < \xi$. This result is consistent with the picture of a percolation-like transition at $p_c = 0.293$. However, in the percolation model, the infinite cluster is known to become compact above p_c. In the present model, we have seen that the open clusters obtained at $p = 0.5$ are fractal, with a fractal dimension which is that of DLA. This non-trivial result shows that the tip effects due to the diffusion dominate the chemical effects due to the nature of the ions. In other words, the self-organized fractal geometry of the DLA model is robust enough not to be affected by the static percolation-like transition driven by the p field.

4. Summary and discussion

In summary, we have studied a DLA model with two species, A and B, for which an A–B growth order is imposed. Intensive numerical simulations were performed with various proportions p of A particles. For $p = \frac{1}{2}$, we observed that about 75% of the clusters grow indefinitely. This percentage decreases with p and becomes zero when a critical value $p_c = 0.293 \pm 0.01$, similar to a percolation threshold, is reached. In the vicinity of this point, a scaling analysis of our numerical data allowed us to compute the critical exponents $\tau = 2.92 \pm 0.06$, $\sigma = 0.71 \pm 0.10$ and $\nu = 0.81 \pm 0.20$. These exponents define a so-far unknown type of critical behaviour. The cluster fractal dimension was found to be the same as in regular DLA, independently of p. This result shows that p governs the mean size of the clusters but that it does not govern their geometry.

Recent experiments have revealed the possibility of growing two-dimensional (2D) irregular crystals of ammonium chloride (NH_4Cl) [8]. The observed growth mechanism (tip-splitting), the measured fractal dimension ($D \simeq 1.67$) and a multifractal analysis [9] all suggest that these crystals are similar to DLA clusters. Although this observation gives more insight into the physical problem, its exact relation with the DLA model remains unclear. As a matter of fact, DLA simulates the case of rapid growth with both vanishing supersaturation

and surface tension. Thus, our model simulates ionic crystal growth in the same limits and the geometry of the NH_4Cl crystals is qualitatively well reproduced (see figure 2).

However, the experiments are performed with a non-zero supersaturation and surface tension effects play a significant role. Saito and Ueta [10] have performed numerical simulations that take these parameters into account. In order to obtain a reasonably realistic model for the above experiments, their approach could be extended to the case of two ionic species. Another possibility would be to adapt a sophisticated solidification model which has been introduced recently [11] to the case of ionic crystal growth. According to this model, a fractal seaweed geometry could be observed, with possibly a fractal dimension different from the DLA value [12]. Nevertheless, there is little hope of discriminating between the two fractal dimensions, at the moment.

In both cases, DLA or fractal seaweed, based on our present results, we would expect that there exists a critical value, $p = p_c$, limiting a fast growth and a slow growth regime. It would thus be interesting to test this point experimentally by growing NH_4Cl crystals from solutions with different NH_4^+ and Cl^- concentrations.

Acknowledgments

It is a pleasure for us to thank H Jamgotchian for his help with data processing and K Kassner for fruitful discussions.

References

[1] Witten T A and Sander L M 1981 *Phys. Rev. Lett.* **47** 1400
[2] Witten T A and Sander L M 1983 *Phys. Rev.* B **27** 5686
[3] Vicsek T 1992 *Fractal Growth Phenomena* 2nd edn (Singapore: World Scientific)
[4] Sevšek F, Debierre J-M and Turban L 1983 *J. Phys. A: Math. Gen.* **16** 801
[5] Meakin P 1987 *Phase Transitions and Critical Phenomena* vol 12 ed C Domb and J L Lebowitz (New York: Academic)
[6] Stauffer D and Aharony A 1992 *Introduction to Percolation Theory* 2nd edn (London: Taylor and Francis)
[7] Bradley R M, Strenski P N and Debierre J-M 1992 *Phys. Rev.* A **45** 8513
[8] Honjo H, Ohta S and Matsushita M 1986 *J. Phys. Soc. Japan* **55** 2487
[9] Ohta S and Honjo H 1987 *Phys. Rev. Lett.* **60** 611
[10] Saito Y and Ueta T U 1989 *Phys. Rev.* A **40** 3408
[11] Ihle T and Müller-Krumbhaar H 1993 *Phys. Rev. Lett.* **47** 1400
[12] Kassner K and Brener E 1993 *Phys. Rev.* E **70** 3083